Survey of Magnetospheric Line Radiation (MLR) events observed by the DEMETER spacecraft

F. Němec[1,2,3], M. Parrot[1], O. Santolík[3,2], C. J. Rodger[4], M. J. Rycroft[5], M. Hayosh[3], D. Shklyar[6], A. Demekhov[7]

Abstract. Magnetospheric Line Radiation (MLR) events are electromagnetic waves in the frequency range between about 1 and 8 kHz that, when presented as a frequency-time spectrogram, take the form of nearly parallel and clearly defined lines which sometimes drift slightly in frequency. They have been observed both by satellites and ground-based

---

F. Němec, LPC2E/CNRS, 3A Avenue de la Recherche Scientifique, 45071, Orléans Cedex 2, France

[1]LPC2E/CNRS, Orléans, France.

[2]Faculty of Mathematics and Physics, Charles University, Prague, Czech Republic.

[3]Institute of Atmospheric Physics, ASCR, Prague, Czech Republic.

[4]Department of Physics, University of Otago, Dunedin, New Zealand.

[5]CAESAR Consultancy, Cambridge, UK.

[6]Space Research Institute (IKI), Moscow, Russia.

[7]Institute of Applied Physics, Russian Academy of Sciences, Nizhny Novgorod, Russia.

instruments, but their origin is still unclear. We present a survey of these MLR waves observed by the DEMETER spacecraft (at an altitude of about 700 km). Three years of VLF Survey mode data were manually searched for MLR events, creating the largest event satellite database of about 650 events, which was then used to investigate the wave properties and geographical occurrence. Finally, the most favorable geomagnetic conditions (Kp and Dst indices) for the occurrence of MLR events have been found. It is shown that MLR events occur mostly at $L > 2$ (upper limit is given by a limitation of the spacecraft), they occur primarily inside the plasmasphere and there is a lower number of events occurring over the Atlantic Ocean than elsewhere on the globe. The MLR events occur more often during the day and usually during, or after, periods of higher magnetic activity. Their frequencies usually lay between about 2 and 6 kHz, with the total frequency bandwidth of an observation being below 2 kHz in the majority of cases. Moreover, it is shown that the longitudinal dimensions of the MLR events can be as large as 100 degrees and they can last for up to a few hours. Finally, we discuss a possibility that MLR events may be triggered by Power Line Harmonic Radiation (PLHR) and we report an event supporting this hypothesis.

1. Introduction

When represented in the form of frequency-time spectrograms, electromagnetic waves observed in the magnetosphere sometimes consist of several clear lines, nearly equidistant in frequency and with a rather slow frequency drift. Such emissions are usually called Magnetospheric Line Radiation (MLR). They have been reported both in ground observations [e.g. *Rodger et al.*, 1999, 2000; *Manninen*, 2005] and low-altitude satellite data [e.g. *Bell et al.*, 1982; *Rodger et al.*, 1995; *Parrot et al.*, 2005; *Němec et al.*, 2007a]. However, their origin is still unknown.

A careful analysis of satellite observations of such events with a line structure [*Němec et al.*, 2007a] showed it was possible to distinguish clearly a class of events called Power Line Harmonic Radiation (PLHR). These events are believed to be generated by electric power systems on the ground and are quite well understood [*Němec et al.*, 2006, 2007b, 2008]. They can be distinguished from MLR events by their frequency spacings corresponding exactly to 50 or 60 Hz and by very small line bandwidth (less than 3 Hz in the majority of cases, as reported by *Němec et al.* [2008]).

Parrot et al. [2007] reported a case-study of a large-scale MLR event. They used simultaneous observations on the ground and also on board a low altitude satellite to demonstrate the enormous size (area of about $7,400,000$ km^2) and time duration (2 hours) of the event. Finally, they hypothesized that the MLR are due to PLHR propagating in the ionosphere and the magnetosphere and undergoing a nonlinear wave-particle interaction in the equatorial plane.

Similarly, *Bullough* [1995] discussed the possibility that MLR originates as PLHR. This concept was further investigated by *Nunn et al.* [1999] using numerical simulations.

In this paper we report upon a survey of 657 MLR events observed by the DEMETER spacecraft, their properties and occurrence. Section 2 describes the DEMETER spacecraft and the wave experiment on board as well as the method of identification of the events. The statistical results obtained are presented in Section 3. Section 4 reports an observation of MLR and PLHR events during the same half-orbit. The results are discussed in Section 5 and summarized in Section 6.

2. Data set and processing

Data from the DEMETER spacecraft have been used in the present study. DEMETER is a French micro-satellite launched in late June, 2004 into a nearly circular orbit with an altitude of 710 km [*Parrot*, 2006]. The altitude of the orbit was decreased to 660 km in December, 2005. Due to the Sun-synchronous orbit DEMETER always records data either around the time of the local day (10:30 LT) or local night (22:30 LT), and for all geomagnetic latitudes lower than 65 degrees. Among several instruments placed on board (electric and magnetic field measurements, plasma analyzer, energetic charged particle detector and Langmuir probe), we have focused only on the analysis of VLF (frequencies lower than 20 kHz) electric field data [*Berthelier et al.*, 2006]. The satellite's normal Survey mode, which is the most common operational state, provides us with power spectrum of one electric field component computed onboard. The frequency resolution is 19.53 Hz and time resolution is 2 s or 0.5 s, depending on the configuration of the instrument. In the Burst mode of the satellite, which is active only above some specific geographic areas, the electric field instrument provides us with a waveform of one electric field component (sampling frequency 40 kHz). The Burst mode is very useful, because it allows us to perform a detailed analysis. However, for a systematic survey of MLR events we are forced to use the Survey mode, because it is used around all the orbit (below 65 degrees geomagnetic latitude) and its occurrence is not limited to any specific areas.

An example of a frequency-time spectrogram of the power spectral density of electric field fluctuations corresponding to an MLR event is shown in Figure 1. Two MLR events can be clearly seen at frequencies between about 2.5 and 4 kHz. MLR is first observed at around an L of 2.6 in the southern hemisphere, continues to be visible as the spacecraft moves equatorwards to L=1.2, and reappears in the northern conjugate hemisphere at an L of about 1.2. Given that the MLR event is seen in both hemispheres at conjugate locations which are only separated by a small amount in longitude and time, we assume that these two MLR events are due to the same source.

We have analyzed the first 3 years of DEMETER data (up to the end of July, 2007), which represents 26036 half-orbits (each DEMETER orbit consists of two half-orbits: "down" or "0" that occurs in the local day and during which the satellite moves approximately from North to South and "up" or "1" that occurs in the local night and during which the satellite moves approximately from South to North). For each of the half-orbits, we have manually checked for the presence of MLR events. In order to do so, frequency-time spectrograms similar to the one from Figure 1 were prepared and visually inspected. The plotted frequency range spans from 1 to 8 kHz and the time covers all the half-orbit (approximately 35 minutes). The color scale used ranged between -3 and $2 \log \left(\mu\mathrm{V}^2\ \mathrm{m}^{-2}\ \mathrm{Hz}^{-1}\right)$ (i.e., minimum to maximum values) and was the same for all the plotted spectrograms. For each of the identified MLR events, we recorded its frequency-time interval (frequency resolution 200 Hz, time resolution 1 minute). MLR events have been found in 549 half-orbits (out of the 26036 analyzed). Altogether, we have identified 657 MLR events. The reason why the total number of identified MLR events is larger than the number of half-orbits containing these events is that there can be two MLR events per one half-orbit, located in the conjugate regions (see Section 5 for a more detailed discussion). An example of this situation was shown in Figure 1.

3. Statistical results

Our large database of the MLR events enabled us to analyze in detail their occurrence and properties. Our main interest was to answer the following questions: Where do the MLR events occur? When do they occur (or, in other words, what are the most favorable conditions for them to occur)? What are their properties?

3.1. Where do the MLR events occur?

We have constructed an occurrence map of the MLR events (Figure 2), which represents positions of all the observed MLR events in geomagnetic dipole coordinates. The latitudinal resolution used was 10 degrees, being the same as the used longitudinal resolution. The reason for using geomagnetic coordinates is that MLR events might propagate along geomagnetic field lines into the opposite hemisphere. Geomagnetic coordinates allow a simple check to be made that the regions are conjugate: they are located at the same geomagnetic longitudes and their geomagnetic latitudes have opposite signs. The lack of events at large geomagnetic latitudes is caused by the fact that DEMETER does not operate at geomagnetic latitudes larger than 65 degrees (see Section 2). It is evident that MLR events occur primarily at larger geomagnetic latitudes and that they occur at all geomagnetic longitudes. However, the number of MLR events occurring over the Atlantic Ocean seems to be lower than the number of events that occur at other geomagnetic longitudes. One can also observe some additional features in Figure 2. For example, there are the peaks in MLR occurrence over Alaska and the Eastern part of Russia. Moreover, there is a peak of MLR occurrence over the region of Antarctica which is the geomagnetic conjugate to North America, but no noticable increase in MLR occurrence is observed above North America itself. This MLR occurrence is discussed in Section 5.

Figure 3 enables us to study the effect of lower number of MLR events observed over the Atlantic Ocean in more detail; in the left panel it shows the probability density of occurrence of MLR events as a function of geomagnetic longitude. The probability of occurrence at geomagnetic longitudes of 0 – 100 degrees is almost half its value at other geomagnetic longitudes. In the right panel the probability density of occurrence of MLR events as a function of geographic longitude is depicted.

Figure 4 shows the range of L-shells at which the MLR events are observed. The left part of the figure represents the probability density of occurrence of MLR events as a function of L-shell; it shows that most of the events are observed at L-values between 2 and 5. This plot was constructed in such a way that for each of the MLR events a counter was increased in all the L-value bins that correspond to the range of L-values of the event. The right part of the figure represents a histogram of the extent of MLR events expressed in L-shells. It is clear that most of the MLR events have L-extent between about 1 and 3 R_E. The L-values were calculated using both the internal and external magnetic field models (N. A. Tsyganenko, http://nssdcftp.gsfc.nasa.gov/models/magnetospheric/tsyganenko).

Further, we have checked whether the L-shells where MLR events are observed correspond to the locations inside or outside the plasmasphere. Figure 5 shows the L-shells of MLR events as a function of the model location of the plasmapause taking into account the geomagnetic activity [*Moldwin et al.*, 2002] at the time of the observation. The central L-shells of the MLR events are plotted as dots and their L-extents are marked by the vertical lines. Moreover, the mean values of the central L-shells of the MLR events for each interval of the model location of the plasmapause are over-plotted by a thick red line. Six intervals of the model L-values have been chosen, spanning from L-values of 2.5 up to 5.5. It can be seen that the MLR events occur inside the plasmasphere (bottom right part of the figure, below the thick diagonal line). Some of them seem to reach beyond, but this could be well explained by the inaccuracies of the model of the plasmapause location, as it is discussed in Section 5.

3.2. When do the MLR events occur?

Further, we have analyzed when the MLR events occur – or, in other words, what are the most favored natural conditions for their occurrence. We have checked whether there is a difference in their occurrence rate between daytime and nighttime (due to the specific orbit of the DEMETER spacecraft, there are just these two possibilities, see Section 2 for more details). It turns out that among the 657 observed events, 390 events occurred during the day and 267 events occurred during the night. Among the 549 half-orbits containing MLR events, 321 were day-time half-orbits and 228 were night-time half-orbits. Therefore, the MLR events seem to occur more frequently during the day than during the night. We can evaluate the statistical significance of this difference simply by using a binomial distribution. If the probability that an MLR event occurs during the day were the same as the probability that an MLR event occurs during the night, the mean number of events occurring during the day $\overline{N_d}$ would be equal to the mean number of events occurring during the night $\overline{N_n}$:

$$\overline{N_d} = \overline{N_n} = p\,N_{total} = 328.5 \quad (1)$$

where $N_{total} = 657$ is the total number of the observed MLR events and $p = 0.5$ is the probability that an MLR event occurs during the day/night supposing it is the same for the two. The appropriate standard deviation can be calculated as follows:

$$\sigma = \sqrt{p\,(1-p)\,N_{total}} \approx 12.8 \quad (2)$$

The difference between the number of events that occur during the day and the number of events that occur during the night therefore corresponds to about 4.8 standard deviations. If we perform the same calculation for the number of half-orbits containing MLR events, we find out that the difference corresponds to about 4.0 standard deviations. As such the preference for daytime MLR events appears highly statistically significant.

It is of a great importance to investigate whether the geomagnetic conditions during the occurrence of MLR events differ from the normal ones or not. We have therefore used the superposed epoch analysis in order to find out what is the dependence of the value of Kp index on the time relative to the time of the MLR events. The time resolution used for the analysis was set to one hour. The results are shown in Figure 6. The left panel represents the dependence obtained for the mean value of Kp index while the right panel represents the same dependence obtained for its median value. Moreover, there is a standard deviation of the mean value σ_M marked by thin lines in the left panel. This is calculated as:

$$\sigma_M = \frac{\sigma}{\sqrt{N}} \tag{3}$$

where σ is the standard deviation of the distribution of Kp values and N is the number of averaged values. It can be seen that there is a statistically significant increase of Kp index a few days before the time of the MLR events. However, the absolute value of the increase is rather low, less than the standard deviation σ, and it becomes statistically significant only due to the large number of analyzed events (see Section 5).

Figure 7 shows by a bold solid line a histogram of Kp indices at the time of the maximum difference from the normal values obtained by the superposed epoch analysis (35 hours before the time of MLR events, mean value of Kp 2.5). For a comparison, a histogram of Kp indices that occurred during all the analyzed period of 3 years is plotted by a thin dotted line. It can be seen that the histogram of Kp indices shortly before the MLR occurrence is slightly shifted towards the larger values.

Figures 8 and 9 represent the same dependence as Figures 6 and 7, but this time for Dst indices. From Figure 9, it can be seen that the distribution of Dst is shifted slightly towards lower values (17 hours before the time of MLR events, mean value of Dst -23.7). This is further confirmed by Figure 8 which shows that there is a decrease of the Dst index for a few days before the time of occurrence of the MLR events. Similarly to Figure 6, the decrease of the mean Dst value is statistically significant, but its absolute value is lower than the standard deviation of the distribution of Dst indices (again, see a detailed discussion in Section 5).

3.3. What are the properties of the MLR events?

The frequencies of observed MLR events are plotted in the left panel of Figure 10. Similarly to the left panel of Figure 4, this plot was constructed in such a way that for each of the MLR events we have increased a counter in all the bins in the range of frequencies corresponding to this event. Most of the events occurred at frequencies between 2 and 6 kHz. The frequency bandwidth of the events, shown in the right panel of Figure 10, is less than 2 kHz in most of the cases.

Checking the number of consecutive half-orbits that contain MLR events enables us to obtain a lower estimate of their longitudinal dimensions, as well as a lower estimate of their time duration (see Section 5). The results are plotted in Figure 11. Individual bins of the histogram correspond to the 1, 2, 3, 4 and 5 consecutive half-orbits of the same direction (up or down) containing MLR events, respectively. On the lower x-axis, these are converted directly to the longitudinal dimension, in degrees, while on the upper x-axis these are converted directly to the time duration, in hours. It can be seen that the longitudinal dimensions may be rather large, up to about 100 degrees, and that the events can last for a few hours.

4. Is an MLR event triggered by PLHR?

In this section we report on a special kind of event, which consists of the observation of an MLR event and Power Line Harmonic Radiation (PLHR) during the same half-orbit, in conjugate hemispheres. The natural question therefore arises: does this represent a case of an MLR event triggered by PLHR? (See a more detailed discussion in Section 5). Figure 12 represents a frequency-time spectrogram of all the entire half-orbit. The PLHR event occurred in the northern hemisphere and was observed approximately between 08:01:30 UT and 08:04:30 UT at frequencies between 2800 and 3600 Hz. The MLR event occurred in the conjugate region and was observed approximately between 08:31:00 UT and 08:36:00 UT at frequencies between 3200 and 4000 Hz. The MLR event was significantly more intense than PLHR event, which is in a good agreement with the statistical results reported by *Němec et al.* [2007a].

The left panel of Figure 13 shows a detailed frequency-time spectrogram of the PLHR event from Figure 12. A set of horizontal lines can be clearly identified. Moreover, DEMETER was in the Burst mode during the observation, which allows us to construct a detailed power spectrum. This is shown in the right panel of Figure 13. Several peaks corresponding to the PLHR lines can be seen. They occur at frequencies of: 2950 Hz, 3000 Hz, 3050 Hz, 3150 Hz, 3250 Hz, 3350 Hz, 3450 Hz, 3550 Hz and 3650 Hz, which corresponds to the exact multiples of the fundamental frequency of the electrical power system of 50 Hz (within 1 Hz uncertainty). This well agrees with *Němec et al.* [2006, 2007b], because the PLHR event was observed above Russia, where the frequency of the power grid systems is 50 Hz.

A detailed frequency-time spectrogram of the MLR event from Figure 12 is shown in Figure 14. A set of nearly horizontal thick lines covered by a noisy emission can be seen. The event seems to start at higher frequencies and moves towards the lower frequencies later (closer to the southern auroral zone).

The idea that an MLR event can be triggered by PLHR is rather old [*Bullough*, 1995; *Nunn et al.*, 1999], but up to now it has lacked a direct experimental verification. This is why the unique measurement shown in Figures 12, 13 and 14 of an MLR event and a PLHR event that occurred during the same half-orbit is important. Located in conjugate regions, the PLHR event was detected first. Although it does not provide definite proof that MLR events are triggered by PLHR, it is rather clear that, at least for this particular event, the two phenomena are connected. Moreover, because the origin of PLHR is quite well understood [*Němec et al.*, 2006, 2007b, 2008], it is reasonable to suppose that it is the MLR event which is affected by the PLHR event, and not vice versa.

5. Discussion

A crucial factor when performing a systematic surveys like that presented here is the method of constructing the database of events. There are two basic possibilities for how to identify interesting events in large data sets. The first of them is to develop an automatic procedure for their identification using some precisely given criteria. The second possibility is to perform a visual inspection and a manual identification of the events. We have chosen the second method for the two reasons: 1) MLR events are quite difficult phenomena to describe and quantify precisely, which makes the development of an automatic procedure very difficult, and 2) an automatic procedure – even if developed – is unlikely to work as well as a trained human eye and mind, and would therefore miss many of the events. The performed manual identification of the events is, in this sense, ideal; however, it is based on the "individual feeling" of the observer and cannot be precisely quantified. This problem was at least partly solved by inspecting the data twice, independently, which we believe practically excludes any false identifications. Further, a constant color scale of the power spectral density spanning from -3 to $2 \log \left(\mu\mathrm{V}^2\ \mathrm{m}^{-2}\ \mathrm{Hz}^{-1}\right)$ has been used in order be consistent all over the analyzed data set. The checked frequency range was also the same for all the half-orbits, spanning from 1 to 8 kHz. Had any events that had occurred outside this frequency range, they would have remained undetected. Although we do not completely exclude the possibility that some MLR events might occur at lower/larger frequencies, the left panel of Figure 10 strongly suggests that, if there are any such events, there are only few of them.

MLR events have been identified in 549 half-orbits among 26036 analyzed. Their occurrence rate is therefore only a bit larger than 2%, meaning that MLR events are not a common phenomenon. There can be two MLR events occurring during a single half-orbit (located in the conjugate regions), resulting into the total number of identified MLR events being equal to 657. Although MLR events are believed to propagate along geomagnetic field lines, bouncing back and forth between the hemispheres, among the 549 half-orbits with MLR events there were only 108 half-orbits with MLR events occurring in the both hemispheres. This has two different explanations, acting simultaneously: 1) DEMETER does not encounter the conjugate points of exactly the same magnetic field line, so that it may miss one MLR event, or 2) at the time when DEMETER is in the conjugate region, the MLR event has already stopped.

The three years of the data analyzed represent a sufficiently large data set required to perform a systematic survey. While there is a limitation due to the technical operation of the DEMETER spacecraft, namely that it does not make observations at geomagnetic latitudes larger than 65 degrees, we can see from Figure 2 and Figure 4 that the MLR events detected are not very much affected by this limitation, because the number of MLR events seems to be decreasing rapidly at larger geomagnetic latitudes.

The results from Figures 2 and 3 show that there is a lower number of MLR events occurring at geomagnetic longitudes corresponding to the Atlantic Ocean. We propose two possible explanations for this effect. The first is that, in the drift loss cone, East of the South Atlantic geomagnetic anomaly, there are insufficient energetic electrons needed to generate the MLR events. In order to support this hypothesis, we can compare the probability density of occurrence of MLR events as a function of geographic longitude shown in the right panel of Figure 3 with electron fluxes as a function of geographic longitude obtained by *Asikainen and Mursula* [2008]. It can be seen that – going from the West – the MLR occurrence starts to decrease at about -90 degrees of geographic longitude. This corresponds well to the area of increasing precipitating electron flux. The MLR occurrence reaches its minimum between -60 and 0 degrees of geographic longitude, corresponding to the peak precipitating electron flux. Afterwards, it slowly increases up to about 120 degrees of geographic longitude, meaning that the occurrence of MLR events seems to be affected by the South-Atlantic Anomaly much further to the East than the precipitating electron flux region. This could be caused by the fact that even after the massive precipitation of electrons stopped, it takes some time to fill-up the slot region again. The second explanation is that at the geomagnetic longitudes of the Atlantic Ocean there are no industrialized areas. Supposing that the generation of MLR events needs a trigger in the form – for instance – of PLHR, the absence of PLHR at these longitudes would explain also the absence of MLR events. It is even possible that both explanations are valid and act together. However, since the area with the lower occurrence rate of MLR events extends well into the geomagnetic longitudes of Europe, the first explanation seems to be the more probable.

The main purpose of Figure 4 was to demonstrate the enormous range of L-shells which can be affected by MLR emissions. Moreover, the typical range of an individual MLR event is rather large, usually about 2 L-shells, but occasionally spanning up to more than

5 L-shells. This clearly indicates that, during the time of their existence, MLR events could affect a huge volume of space in the inner magnetosphere.

Figure 5 shows the position of MLR events with respect to the plasmapause. Because no direct measurements are available, we have used the empirical model of *Moldwin et al.* [2002], with two parameters (Kp, MLT), based on data from the CRRES spacecraft. The model is based on the linear best fit to the satellite data. Thus, it expresses the average plasmapause location, but in an individual case it can significantly underestimate (or overestimate) the real location ($\sigma_{L_{pp}} \approx 0.5$ according to *Moldwin et al.* [2002]). Because the scatter of MLR events beyond the plasmasphere observed in Figure 5 is smaller than inaccuracies of the model L_{pp}, the imperfect agreement is most probably caused solely by the inaccuracies in the used model. Moreover, a detailed examination of the events that reach beyond the model location of the plasmasphere reveals that these occurred during low values of the Kp index, but for which the Kp index was quite large about twelve hours before. Since the model of the plasmapause location takes into account the maximum value of the Kp index in the previous 12 hours, it results in a significantly compressed plasmasphere. However, because the present values of Kp are low and because the large value occurred just at the edge of the time interval taken into account by the model, it is reasonable to suppose that the plasmasphere in such cases is compressed much less than predicted. Consequently, there is no strong evidence that MLR events stretch beyond the plasmasphere; it is more likely they are strictly limited to be within the plasmapause.

Figures 6, 7, 8 and 9 show that MLR events occur preferentially during or after periods of larger geomagnetic activity. Although this change in average values of geomagnetic indices (Kp, Dst) is statistically significant, its absolute value is smaller than typical fluctuations of the indices. The observed increase of Kp index is about 0.7, while the Kp index commonly varies between 0 and 5 (see dotted histogram in Figure 7). The observed decrease of Dst index is about 10 nT, while Dst commonly varies between -50 and 10 nT (see dotted histogram in Figure 9). This means that, although the occurrence of MLR events is clearly linked to the increased geomagnetic activity, this connection has been revealed only by using the superposed epoch analysis of a large number of events. It is statistically significant, but for an individual event the value of Kp / Dst can behave rather differently. The physical explanation of this observed dependence is that energetic electrons are needed in order to generate the MLR events. This result presents an evidence that the phenomenon is the result of a wave-particle interaction, probably taking place at the geomagnetic equator (which is the preferred region for such types of interaction *Trakhtengerts and Rycroft* [2008] and, moreover, is well consistent with MLR events often being observed in the conjugate regions).

From the frequency range of MLR events depicted in the left panel of Figure 10 it can be seen that the analyzed frequency band of 1 – 8 kHz was well chosen: the probability density of occurrence of MLR events at frequencies close to 1 kHz and 8 kHz is close to zero. This means that, although there may be some MLR events occurring outside the frequency band analyzed, there are probably only a few of them. It is interesting to compare this frequency range with the frequency range of PLHR and MLR events reported by *Němec et al.* [2007a]. An automatic identification procedure has been used to identify PLHR events in electric field burst-mode data in the frequency range 0.5 – 4 kHz [*Němec et al.*, 2006]. This procedure was also able to identify some events that were classified as MLR events. Altogether, 49 PLHR events and 23 MLR-like events were identified in 1650 hours of burst-mode electric field data. It was shown [*Němec et al.*, 2007a] that PLHR events occur at frequencies between about 1 and 4 kHz, being most frequent between 2 and 3 kHz. MLR-like events were reported at all frequencies below 4 kHz, being more frequent at lower frequencies.

The present study shows that the MLR events occur most frequently at frequencies between about 2 and 4 kHz, which are the frequencies well comparable with the typical frequencies of PLHR. Although MLR events seem to extend to higher frequencies than PLHR, this may be caused by the limited frequency range analyzed by *Němec et al.* [2007a].

There is a significant difference between the frequency range of MLR events reported in the present study and the frequency range of MLR-like events reported by *Němec et al.* [2007a]. This can be explained by taking into account the Figure 7 of *Němec et al.* [2007a] which shows two different classes of MLR-like events: 1) events with frequencies below 1 kHz located close to the geomagnetic equator, and 2) events with frequencies well comparable with PLHR events at larger geomagnetic latitudes. Since the present study focuses solely on the frequency band 1 – 8 kHz, only the events from the second class are identified. The events from the first class, which we believe are naturally generated by instabilities of the ion distribution functions, will be thoroughly discussed in a separate paper.

Figure 11 shows that the longitudinal dimensions of MLR events can reach up to about 100 degrees and that the events can last as long as a few hours. These estimates were determined by evaluating the number of consecutive half-orbits containing the MLR events and so represent a lower estimate of the longitudinal dimensions and time duration. This is due to the fact that there can be two reasons why an MLR event is not observed in the next half-orbit: 1) the MLR event does not extent that far – this is the reason used to find the longitudinal dimensions, or 2) the MLR event does not last long enough to survive until the next DEMETER pass – although it extended far enough during its lifetime, it is not observed, because it had already died at the time of the observation. This reason was used to determine the time duration. Because in reality both these reasons are acting simultaneously, what we obtain is a lower estimate of the longitudinal dimension and the lower estimate of the time duration. There might also occur the situation of two separate MLR events extending not very far in longitude but present at the same time. In such a situation, DEMETER would see one of them during the first pass and the other of them during the second; we would evaluate that situation as an individual MLR event extending over the two half-orbits. However, since MLR events are not so frequent and a special configuration would be required, we can estimate that this possibility is rather unlikely (about 0.04 percent). Finally, we would like to underline once more that the longitudinal and L-range of MLR events, as well as their time duration, can be rather large; when present they could therefore represent an important factor in determining the dynamics of the plasmasphere.

6. Conclusions

The results of a systematic study of observations of MLR events by a low-altitude satellite have been presented. Altogether, 657 events in 549 half-orbits have been identified. According to our knowledge, this represents the largest satellite database of MLR events collected to date. Their occurrence and properties have been thoroughly investigated.

Our results show that MLR events occur mostly at $L > 2$ and that they do not occur outside the plasmasphere. There are fewer events at geomagnetic longitudes corresponding to the Atlantic Ocean. Moreover, the MLR events occur slightly more often during the day than during the night. They usually occur during or after the periods of higher magnetic activity. Most often they are observed at frequencies between 2 and 6 kHz, and their frequency bandwidth is below 2 kHz in the majority of cases. Their longitudinal dimensions can extend up to about 100 degrees and they can last for as long as a few hours. Finally, we have reported the observation of MLR and PLHR events during the same half-orbit. This we have discussed in terms of the possibility that PLHR may serve as a trigger for MLR.

7. Acknowledgements

The work of FN and MP is supported by the Centre National d'Etudes Spatiales (CNES). It is based on observations with the electric field experiment ICE carried on DEMETER. The authors thank CNES personnel involved in the mission development of the French DEMETER satellite, those currently in charge of the operations in Toulouse, and J. Y. Brochot of LPCE/CNRS Orléans for his help with data processing. They thank J. J. Berthelier for the use of electric field data. They acknowledge support of the PICS grant no. 3725 from CNRS/DREI and the LAPBIAT 2 program (contract RITA-CT-2006-025969) from the Sodankylä Geophysical Observatory, Finland.

References

Asikainen, T., and K. Mursula (2008), Energetic electron flux behavior at low L-shells and its relation to the south atlantic anomaly, *J. Atmos. Solar-Terr. Phys.*, *70*, doi:

10.1016/j.jastp.2007.08.061.

Bell, T. F., J. P. Luette, and U. S. Inan (1982), ISEE 1 observations of VLF line radiation in the Earth's magnetosphere, *J. Geophys. Res.*, *87*(A5), 3530–3536.

Berthelier, J. J., et al. (2006), ICE, the electric field experiment on DEMETER, *Planet. Space Sci.*, *54*, 456–471.

Bullough, K. (1995), *Handbook of Atmospheric Electrodynamics*, vol. 2, chap. Power Line Harmonic Radiation: Sources and Environmental Effects, pp. 291–332, CRC Press, Boca Ralton, Fla.

Manninen, J. (2005), *Some Aspects of ELF-VLF Emissions in Geophysical Research*, chap. Magnetospheric Line Radiation, pp. 85–110, 98, Sodankylä Geophysical Observatory Publications, Sodankylä, Finland.

Moldwin, M. O., L. Downward, H. K. Rassoul, R. Amin, and R. R. Anderson (2002), A new model of the location of the plasmapause: CRRES results, *J. Geophys. Res.*, *107*(A11), doi:10.1029/2001JA009211.

Nunn, D., J. Manninen, T. Turunen, V. Trakhtengerts, and N. Erokhin (1999), On the nonlinear triggering of VLF emissions by power line harmonic radiation, *Ann. Geophys.*, *17*, 79–94.

Němec, F., O. Santolík, M. Parrot, and J. J. Berthelier (2006), Power line harmonic radiation (PLHR) observed by the DEMETER spacecraft, *J. Geophys. Res.*, *111*, doi:10.1029/2005JA011480.

Němec, F., O. Santolík, M. Parrot, and J. J. Berthelier (2007a), Comparison of magnetospheric line radiation and power line harmonic radiation: a systematic survey using the DEMETER spacecraft, *J. Geophys. Res.*, *112*, doi:10.1029/2006JA012134.

Němec, F., O. Santolík, M. Parrot, and J. J. Berthelier (2007b), Power line harmonic radiation: A systematic study using DEMETER spacecraft, *Adv. Space Res.*, *40*, 398–403.

Němec, F., O. Santolík, M. Parrot, and J. Bortnik (2008), Power line harmonic radiation observed by satellite: Properties and propagation through the ionosphere, *J. Geophys. Res.*, *113*(A08317), doi:10.1029/2008JA013184.

Parrot, M. (Ed.) (2006), *First Results of the DEMETER Micro-Satellite*, vol. 54, pp. 411–558, Special Issue of Planet. Space Sci.

Parrot, M., F. Němec, O. Santolík, and J. J. Berthelier (2005), ELF magnetospheric lines observed by DEMETER, *Ann. Geophys.*, *23*, 3301–3311.

Parrot, M., J. Manninen, O. Santolik, F. Nemec, T. Turunen, T. Raita, and E. Macusova (2007), Simultaneous observation on board a satellite and on the ground of large-scale magnetospheric line radiation, *Geophys. Res. Lett.*, *34*(L19102), doi: 10.1029/2007GL030630.

Rodger, C. J., N. R. Thomson, and R. L. Dowden (1995), VLF line radiation observed by satellite, *J. Geophys. Res.*, *100*(A4), 5681–5689.

Rodger, C. J., M. A. Clilverd, K. H. Yearby, and A. J. Smith (1999), Magnetospheric line radiation observations at Halley, Antarctica, *J. Geophys. Res.*, *104*(A8), 17,441–17,447.

Rodger, C. J., M. A. Clilverd, K. H. Yearby, and A. J. Smith (2000), Temporal properties of magnetospheric line radiation, *J. Geophys. Res.*, *105*(A1), 329–336.

Trakhtengerts, V. Y., and M. J. Rycroft (2008), *Whistler and Alfvén mode cyclotron masers in space*, p. 354, Cambridge University Press.

Figure 1. An example of a frequency-time spectrogram of a single half-orbit used for the identification of MLR events. Two MLR events at frequencies between about 2.5 and 4 kHz can be clearly seen, located in magnetically conjugate regions.

Figure 2. Map of occurrence of MLR events in geomagnetic coordinates. Shown color coded is the number of events observed in a given latitudinal-longitudinal bin.

Figure 3. (Left) Probability density of occurrence of MLR events as a function of geomagnetic longitude. (Right) Probability density of occurrence of MLR events as a function of geographic longitude.

Figure 4. (Left) Probability density of occurrence of MLR events as a function of L-shell. (Right) L-extent of the observed MLR events.

Figure 5. (Dots) Central L-shells of the MLR events as a function of model location of the plasmapause. (Thick red line) Mean values of central L-shells of the MLR events. (Vertical lines) L-extents of the MLR events.

Figure 6. (Left) Bold: Mean value of Kp index as a function of the time relative to the time of MLR events. Thin: Standard deviation of the mean value. (Right) Median value of Kp index as a function of the time relative to the time of the MLR events.

Figure 7. (Solid) Histogram of Kp indices at the time of the maximum difference from the normal values obtained by the superposed epoch analysis. (Dotted) Histogram of Kp indices during all the analyzed 3 years.

Figure 8. (Left) Bold: Mean value of Dst index as a function of time relative to the time of the MLR event. Thin: Standard deviation of the mean value. (Right) Median value of Dst index as a function of time relative to the time of the MLR event.

Figure 9. (Solid) Histogram of Dst indices at the time of the maximum difference from the normal values obtained by the superposed epoch analysis. (Dotted) Histogram of Dst indices during all the analyzed 3 years.

Figure 10. (Left) Frequency range of the observed MLR events. (Right) Frequency bandwidth of the observed MLR events.

Figure 11. Lower estimate of longitudinal dimension of the observed MLR events (bottom x-axis), and lower estimate of time duration of the observed MLR events (upper x-axis).

Figure 12. Frequency-time spectrogram of a half-orbit containing a PLHR event and an MLR event in geomagnetically conjugate regions.

Figure 13. (Left) Detailed frequency-time spectrogram of the PLHR event from Figure 12. (Right) Power spectrum corresponding to the PLHR event from the left part.

Figure 14. Detailed frequency-time spectrogram of the MLR event from Figure 12.

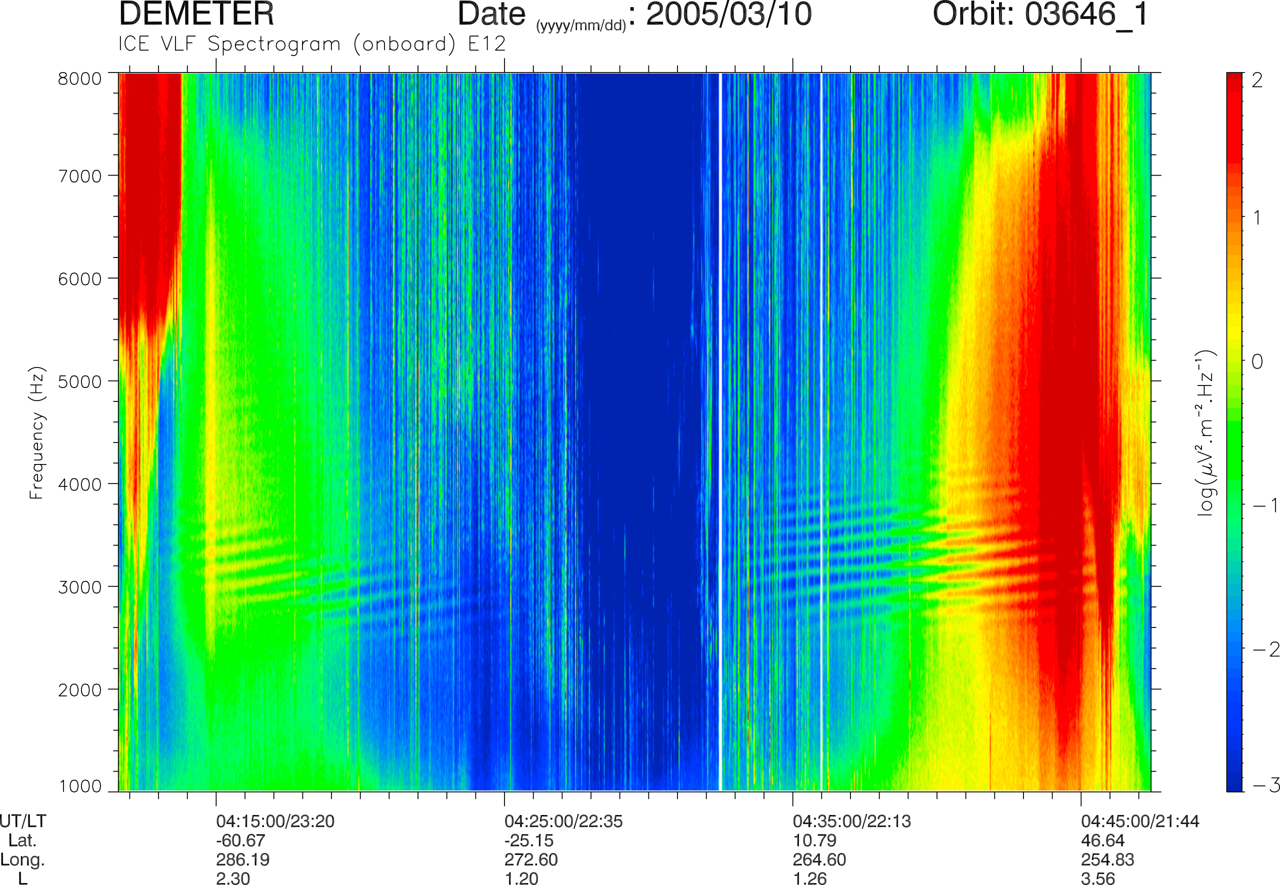
DEMETER
Date (yyyy/mm/dd): 2005/03/10
Orbit: 03646_1
ICE VLF Spectrogram (onboard) E12
Frequency (Hz)
8000
7000
6000
5000
4000
3000
2000
1000
$\log(\mu V^2.m^{-2}.Hz^{-1})$
2
1
0
−1
−2
−3
UT/LT
Lat.
Long.
L
04:15:00/23:20
-60.67
286.19
2.30
04:25:00/22:35
-25.15
272.60
1.20
04:35:00/22:13
10.79
264.60
1.26
04:45:00/21:44
46.64
254.83
3.56

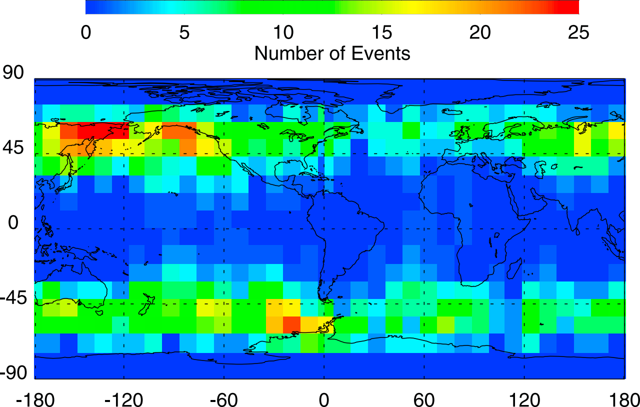

0
5
10
15
20
25
Number of Events
90
45
0
-45
-90
-180
-120
-60
0
60
120
180

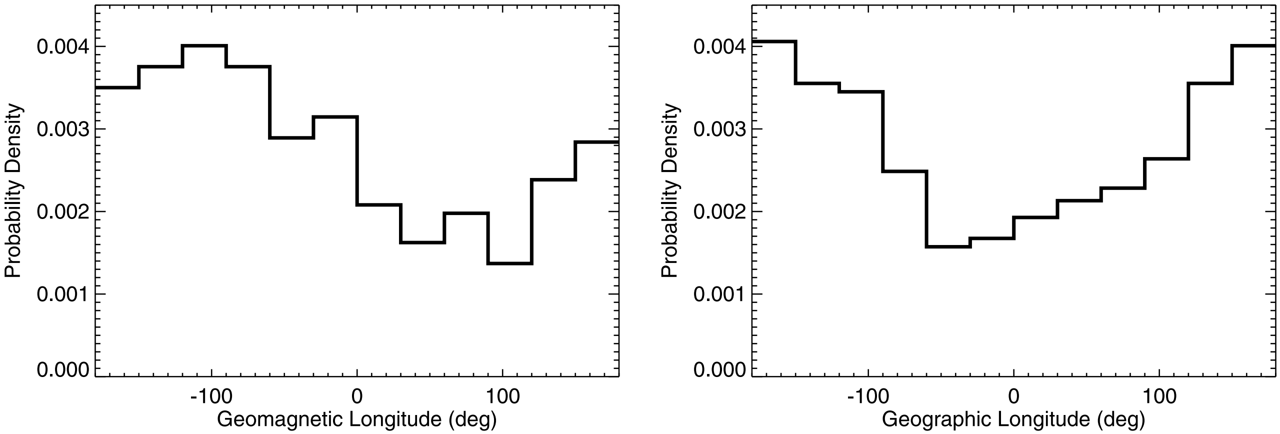

0.004
0.003
0.002
0.001
0.000
Probability Density
-100
0
100
Geomagnetic Longitude (deg)
0.004
0.003
0.002
0.001
0.000
Probability Density
-100
0
100
Geographic Longitude (deg)

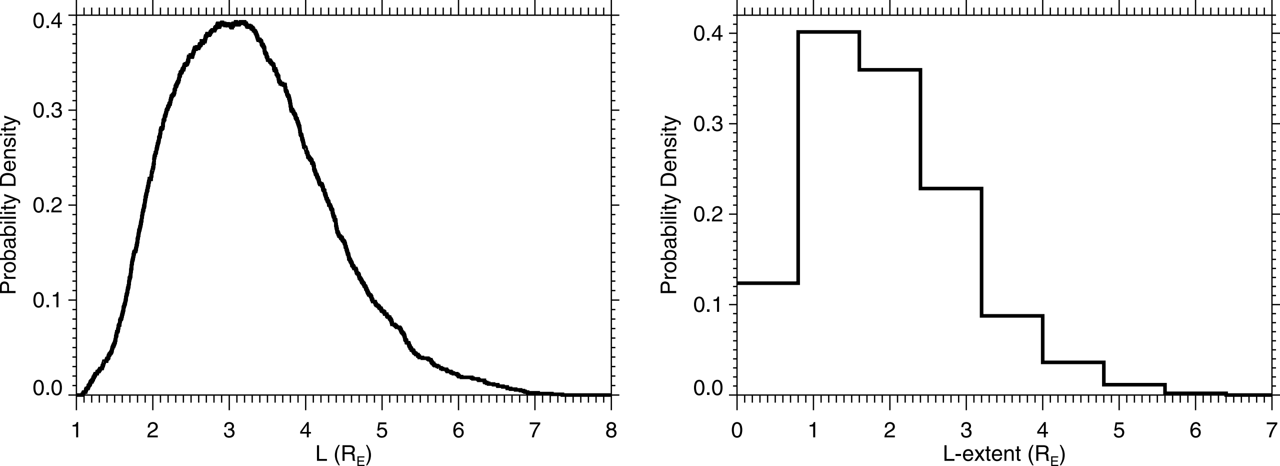
Probability Density
0.0
0.1
0.2
0.3
0.4
1
2
3
4
5
6
7
8
L (R_E)
Probability Density
0.0
0.1
0.2
0.3
0.4
0
1
2
3
4
5
6
7
L-extent (R_E)

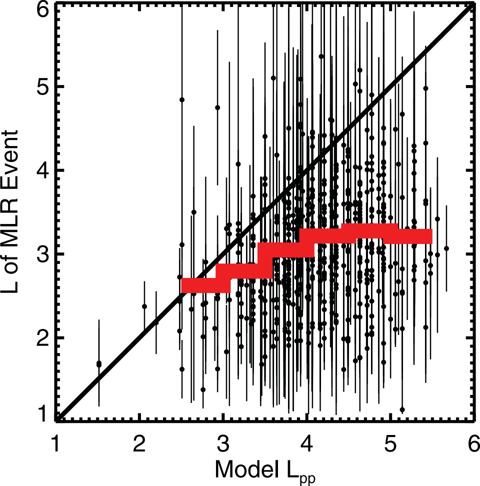

L of MLR Event
Model L_{pp}
1
2
3
4
5
6
1
2
3
4
5
6

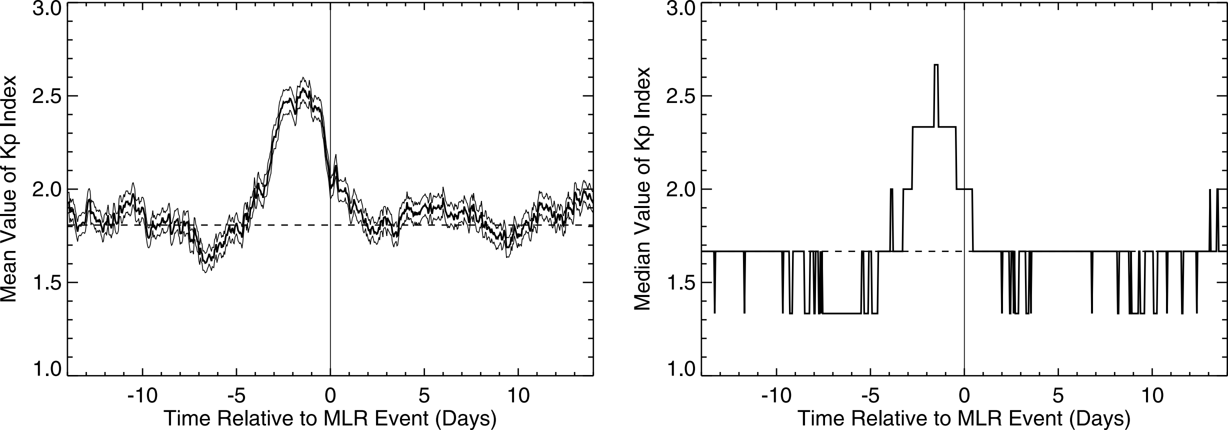
Mean Value of Kp Index
Time Relative to MLR Event (Days)
3.0
2.5
2.0
1.5
1.0
-10
-5
0
5
10
Median Value of Kp Index
Time Relative to MLR Event (Days)

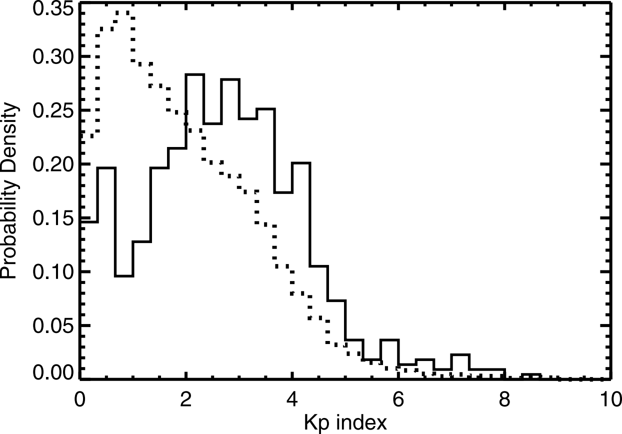

0.35
0.30
0.25
0.20
0.15
0.10
0.05
0.00
Probability Density
0
2
4
6
8
10
Kp index

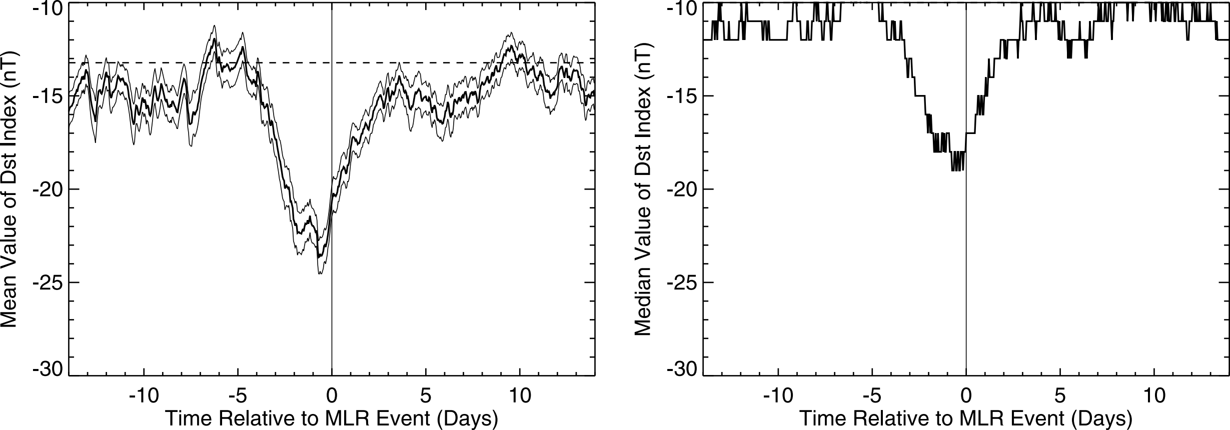

Mean Value of Dst Index (nT)
-10
-15
-20
-25
-30
-10
-5
0
5
10
Time Relative to MLR Event (Days)
Median Value of Dst Index (nT)
-10
-15
-20
-25
-30
-10
-5
0
5
10
Time Relative to MLR Event (Days)

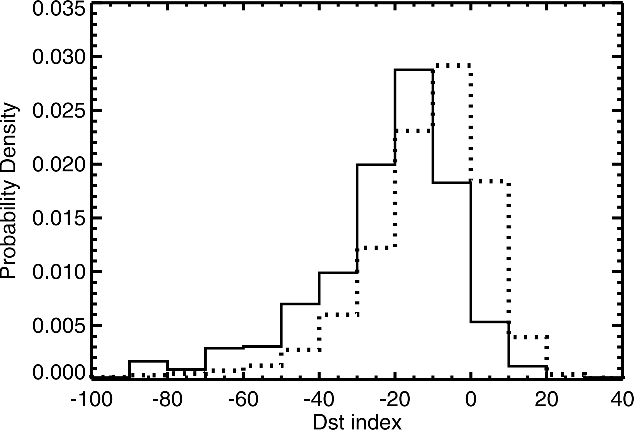

Probability Density
0.035
0.030
0.025
0.020
0.015
0.010
0.005
0.000
-100
-80
-60
-40
-20
0
20
40
Dst index

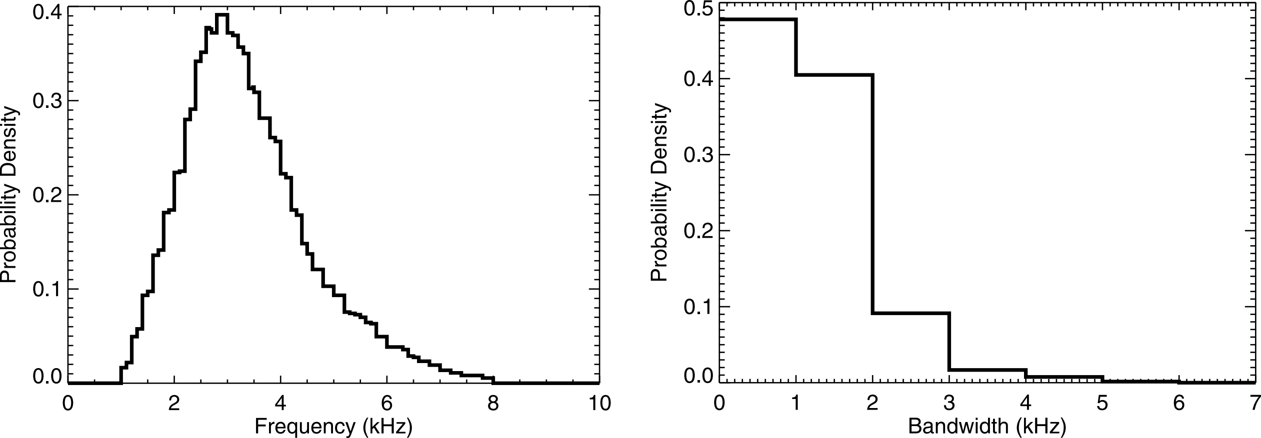

Probability Density
0.0
0.1
0.2
0.3
0.4
0
2
4
6
8
10
Frequency (kHz)
Probability Density
0.0
0.1
0.2
0.3
0.4
0.5
0
1
2
3
4
5
6
7
Bandwidth (kHz)

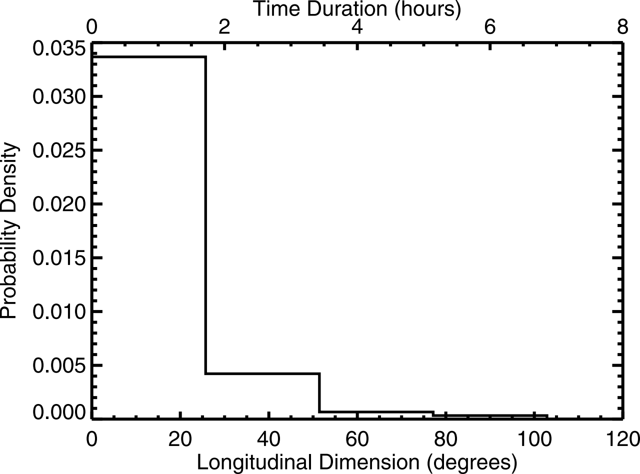

Time Duration (hours)
0
2
4
6
8
0.035
0.030
0.025
0.020
0.015
0.010
0.005
0.000
Probability Density
0
20
40
60
80
100
120
Longitudinal Dimension (degrees)

DEMETER Date (y/m/d): 2007/04/13 Orbit: 14834_0

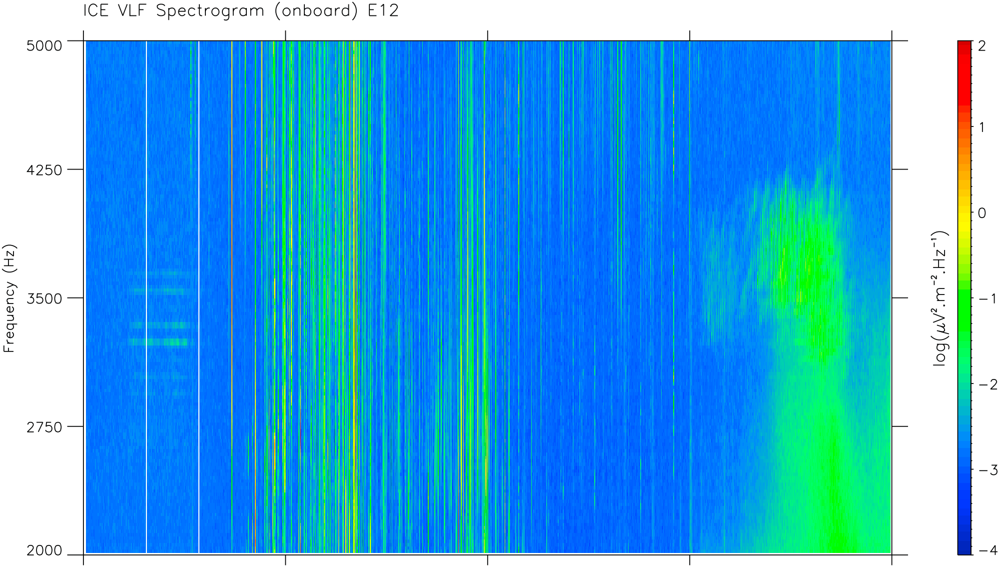

UT/LT	07:59:30/11:51	08:09:07/10:39	08:18:45/10:16	08:28:22/09:54	08:38:00/08:56
Lat.	70.99	36.87	1.90	-33.03	-67.29
Long.	57.94	37.47	29.26	21.33	4.52
L	6.32	1.50	1.10	1.91	4.33

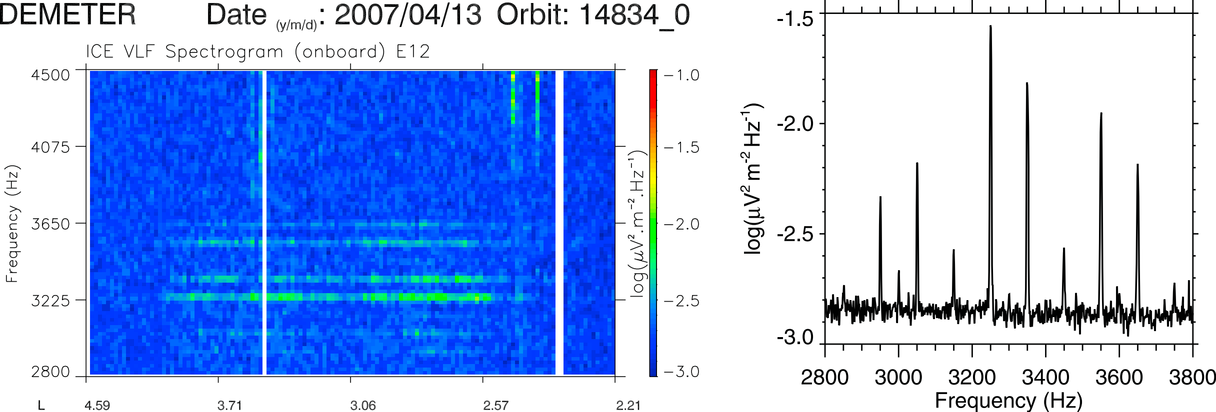

DEMETER Date (y/m/d): 2007/04/13 Orbit: 14834_0
ICE VLF Spectrogram (onboard) E12
Frequency (Hz)
4500
4075
3650
3225
2800
L
4.59
3.71
3.06
2.57
2.21
log(μV².m⁻².Hz⁻¹)
−1.0
−1.5
−2.0
−2.5
−3.0
log(μV² m⁻² Hz⁻¹)
-1.5
-2.0
-2.5
-3.0
2800
3000
3200
3400
3600
3800
Frequency (Hz)

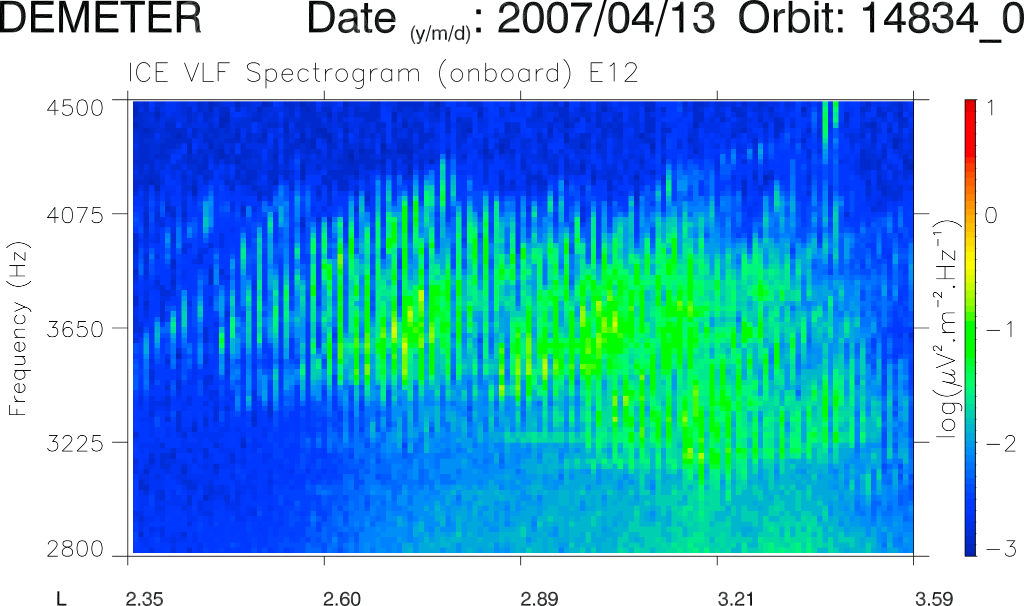
DEMETER Date (y/m/d): 2007/04/13 Orbit: 14834_0
ICE VLF Spectrogram (onboard) E12
Frequency (Hz)
4500
4075
3650
3225
2800
log(μV².m⁻².Hz⁻¹)
1
0
−1
−2
−3
L
2.35
2.60
2.89
3.21
3.59